The 5th International Symposium - Supercritical CO2 Power Cycles
March 28-31, 2016, San Antonio, Texas

High-Temperature Corrosion of Diffusion Bonded Ni-based Superalloys in CO_2

Ömer N. Doğan
Materials Research Engineer
National Energy Technology Laboratory
Albany, OR USA
omer.dogan@netl.doe.gov

Casey Carney
Research Scientist
National Energy Technology Laboratory
and AECOM
Albany, OR USA
casey.carney@netl.doe.gov

Richard P. Oleksak
ORISE Postdoctoral Researcher
National Energy Technology Laboratory
Albany, OR USA
richard.oleksak@netl.doe.gov

Corinne R. Disenhof
Research Scientist
National Energy Technology Laboratory and
AECOM
Albany, OR USA
corinne.disenhof@netl.doe.gov

Gordon R. Holcomb
Materials Research Engineer
National Energy Technology Laboratory
Albany, OR USA
gordon.holcomb@netl.doe.gov

Ömer Doğan is a Materials Research Engineer in the Structural Materials Team in the Research & Innovation Center at NETL. He received his Ph.D. from Case Western Reserve University in Materials Science & Engineering in 1990. Current research focuses on the evaluation and development of heat, corrosion, and wear resistant materials for applications in harsh environments.

Casey Carney received his B.S. in chemistry and engineering physics from Hope College in 1998. He received his Ph.D. in Chemical Engineering from the University of Colorado in 2005, studying the production of fine nickel metal powders via thermal decomposition. He is currently an employee of AECOM as a contractor to NETL. His recent research topics have included: oxy-combustion flame analysis, thermal decomposition kinetics, and materials performance in extreme combustion and sCO_2 environments.

Richard Oleksak is an ORISE Postdoctoral Researcher in the Structural Materials Team in the Research & Innovation Center at NETL. He received his Ph.D. from Oregon State University in Chemical Engineering in 2014. Current research focuses on the understanding of alloy oxidation and corrosion in environments relevant to supercritical CO_2 power cycles.

Corinne Disenhof is a Research Scientist with AECOM under contract to NETL. She received a B.S. in Geology from the University of New Hampshire in 2009. Current projects include research on geologic carbon dioxide storage resources and analytical support of materials and corrosion research.

Gordon Holcomb is a Materials Research Engineer in the Structural Materials Team in the Research & Innovation Center at NETL. He received his Ph.D. from the Ohio State University in Metallurgical Engineering in 1988. Current projects cover corrosion issues in fossil energy systems.

Abstract

Supercritical CO_2 power cycles rely heavily on heat recuperation for increased efficiency. Microchannel heat exchangers are proposed as one option to reduce capital cost, equipment size, and enhance heat transfer between high- and low-temperature working fluids. Microchannel architectures are typically formed by a lamination process wherein channels are formed in layers, which are then stacked and diffusion bonded together. Environmental stability of diffusion bonded regions of Haynes 230 and Haynes 282 stacks was investigated by exposing coupons to CO_2 in a tube furnace at 700°C for 500 hours. After the exposure, mass change of the coupons were determined and the coupons were characterized using XRD, SEM, and EDS. The diffusion bond regions of H230 did not exhibit an accelerated oxidation whereas diffusion bonding of H282 resulted in increased mass gains during oxidation.

Introduction

Due to the potential for improved efficiencies in power generation, interest in sCO_2 cycles has increased in recent years. The sCO_2 cycles rely heavily on heat recuperation for increased efficiency. Compact heat exchanger designs such as microchannel [Ghazvini], printed circuit [Le Pierres], microtubular, plate-fin, wire-mesh [Foursprings], and others are proposed to reduce

equipment size and enhance heat transfer between the high-temperature and low-temperature working fluids in sCO_2 power cycles.

Components containing small features in compact heat exchangers are typically joined together by diffusion bonding or brazing. Likewise, microchannel architectures are formed by a lamination process wherein channels are formed in layers, which are then stacked and diffusion bonded or brazed together. Diffusion bonding is a solid state process that involves pressing layers of metallic materials at high temperatures (usually T > 0.5 * melting point) for several hours. This allows diffusion of species across the contact surfaces of layers eventually forming strong bonding [Hill]. A thin layer of lower melting point alloy with an appropriate composition is placed between the joining surfaces before pressing at high temperatures in the case of brazing. When the stack is heated, this results in a transient liquid phase which facilitates bonding [Cook]. Although the goal is to form a monolithic structure, depending on the alloy composition and microstructure, the interface region of the diffusion bonded or brazed structure may have a chemical composition and microstructure different from the parent alloy. This can be a source of mechanical and/or chemical instability for the structure in the application environments. Sometimes, post diffusion bonding heat treatment may be practical to eliminate or reduce the chemical gradient and microstructural variation in the structure.

This paper examines the effects of a high-purity CO_2 atmospheric pressure environment on the diffusion bonded regions of two Ni-based alloy stacks and compares them to the high-temperature oxidation behavior of the parent materials, namely Haynes 230 and Haynes 282. While high pressure exposure in supercritical CO_2 is preferred, a survey of exposure tests at high pressures [Holcomb] has shown, for Ni-base alloys, little effect from pressure on oxidation kinetics or scale oxide morphologies. The longest of these tests was 3000 h [Lee]; it is possible that differences with pressure will emerge after very long-term exposures.

Experimental Procedure

Haynes 230 (H230) and Haynes 282 (H282) alloys were acquired in sheet form (0.533 mm and 0.584 mm thick, respectively). The nominal alloy compositions are given in Table 1. The sheets were cut into 38.1 mm square pieces using a water jet cutter. The square pieces were cleaned and half of the pieces for each alloy were nickel plated (3 µm thick) using an electroless process. One hundred pieces (layers) were stacked to form Ni-plated and non-Ni-plated stacks of each alloy. The stacks were diffusion bonded in a vacuum chamber at 1150°C for 8 hours under a uniaxial pressure of 12.7 MPa. The diffusion bonding was successful for the H230 Ni-plated and non-Ni-plated, and H282 Ni-plated stacks. The H282 non-Ni-plated stack did not bond. See Kapoor (Paper # 075 in this symposium) for more details on the diffusion bonding process and

characterization of the diffusion bonded samples prior to exposure in CO_2. No post diffusion bonding heat treatment was applied to the stacks.

Table 1. Nominal chemical composition (weight %) of materials used in this study (Haynes 230 and Haynes 282).

	Ni	Cr	W	Ti	Mo	Fe	Co	Mn	Si	Al	C	B
H230	57	22	14	--	2	3*	5*	0.5	0.4	0.3	0.10	0.015*
H282	57	19.5	--	2.1	8.5	1.5*	10	0.3*	0.15*	1.5	0.06	0.005

*Maximum

Corrosion coupons (15 mm x 10 mm x 1 mm) were machined from the stacks such that each coupon contained approximately 25 bonded layers as shown schematically in Fig. 1. Surfaces were ground to a 600 grit (CAMI, Coated Abrasive Manufacturers Institute, now part of the Unified Abrasives Manufacturers' Association) finish. The samples were then ultrasonically cleaned in isopropyl alcohol, dried, and weighed. The coupons were designated by alloy designation (H230 or H282), DB if they were machined from the diffusion bonded stacks, and Ni if the alloy layers were plated with nickel before the diffusion bonding. Coupons without DB or Ni designations were machined from the as-received alloy sheets and were not diffusion bonded. The coupons prepared from the as received materials of H230 and H282 had a thickness of the sheet. They were exposed with their as-received surface roughness (R_a of 353 nm for H230 and 161 nm for H282).

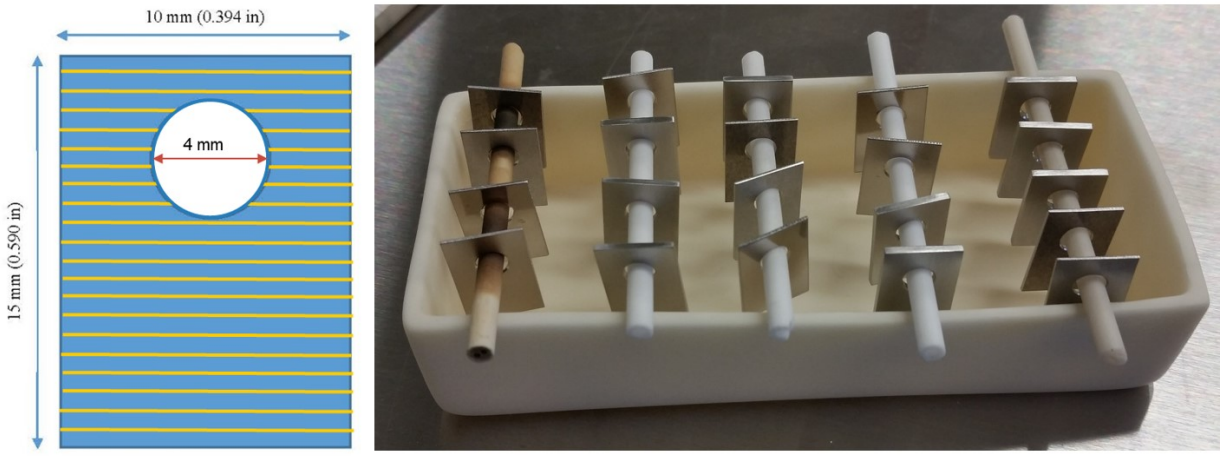

Figure 1: Geometry of test coupons used in oxidation tests (Left). The coupons were machined from diffusion bonded stacks. The coupons are shown prior to the test as they were placed in the furnace tube (Right).

The coupons were exposed to ambient pressure CO_2 at 700°C for 500 hours. The exposures were performed in a horizontal tube furnace, inside an alumina tube. The tube inside diameter was 6.81 cm. The sample rack and samples are shown in Fig. 1. Carbon dioxide, with a purity of 99.999%, was fed into the tube chamber at a rate of 269 cm^3/min, or 0.032 kg/hr. At test conditions this resulted in a fluid velocity of 25 cm/min through the furnace tube, which corresponded to a test section volume change every 12 s. After the coupons were placed in the furnace tube and the tube was sealed, the CO_2 flow was started 24 hours before the heating was begun.

The exposed coupons were weighed using a balance capable of measuring 10^{-5} grams to determine the mass change. X-ray diffraction (XRD) was used to determine the compounds forming on the surface of the coupons due to exposure. The XRD apparatus was a Rigaku Ultima III. Copper K_α characteristic radiation was used to scan a 2Θ range of 10° to 100° with a 0.02° step size. An FEI Inspect scanning electron microscope (SEM) with energy dispersive spectroscopy (EDS) capabilities was used to obtain images and microchemical data on the exposed surfaces and cross-sections. A JEOL 7000F SEM equipped with wavelength dispersive spectroscopy (WDS) was used for H230-DB-Ni cross-sections to avoid the convolution of W and Si peaks in EDS spectra. The contrast/brightness of X-ray maps were enhanced to emphasize features of interest and thus should not be regarded as quantitative.

Results and Discussion

Average mass change for the parent alloy and diffusion bonded coupons after 500 h exposure to CO_2 at 700°C is given in Table 2. The H230 and H282 monolithic coupons showed similar mass gains which were less than that of the diffusion bonded coupons. The diffusion bonded coupons of H282 gained approximately twice as much mass than the diffusion bonded coupons of H230. The coupons of diffusion bonded Ni-plated and non-Ni-plated H230 exhibited similar mass gains.

Table 2. Mass changes as a result of the CO_2 exposure at 700°C for 500 h. Averages and standard deviations are from three coupons for each condition.

	Average mass change (mg/cm^2)	Standard deviation (mg/cm^2)
H230	0.077	0.012
H230-DB	0.115	0.013
H230-DB-Ni	0.112	0.005
H282	0.038	0.022
H282-DB-Ni	0.236	0.008

XRD spectra acquired from the exposed specimens are shown in Figs. 2 and 3 for the H230 and H282 coupons, respectively. All spectra in Fig. 2 show predominantly the peaks from the fcc matrix and the secondarily peaks from the M_6C phase (where M is primarily W and Ni). The matrix and carbides are the two major phases present in H230. The rest of the peaks on the spectra are from a phase formed during the exposure which was identified as Cr_2O_3.

Fig. 3 shows the XRD spectra acquired from the H282 coupons. The largest peaks represent the fcc matrix phase. The other major phase in the H282 base alloy is γ', in the form of small precipitates, which did not yield any identifiable peaks in the diffraction pattern. This may partly be due to having a γ'-precipitate free zone under the external oxidation scale as observed in the SEM images (Fig. 7c, f). However, other researchers have encountered similar results with H282, where γ' is undetectable by XRD but visible with SEM [Pérez-González].

The major oxide phase detected on the exposed H282 and H282-DB-Ni specimens was Cr_2O_3. TiO_2 (rutile) has been observed in XRD results for previous CO_2 exposures [Holcomb], but here its presence is only suggested by the XRD in H282-DB-Ni by a very small primary peak and an increased intensity in the Cr_2O_3 secondary peak, which overlaps the TiO_2 secondary peak. As shown later, SEM results also support the presence of a small amount of TiO_2 present in H282-DB-Ni (Fig. 6).

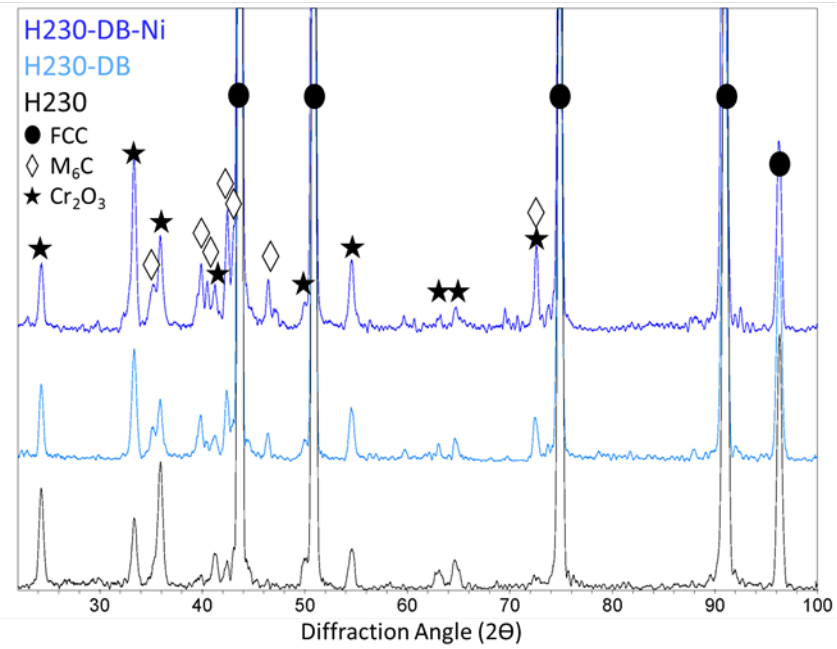

Figure 2: XRD spectra from the exposed surfaces of H230 (black), H230-DB-Ni (dark blue), and H230-DB (light blue).

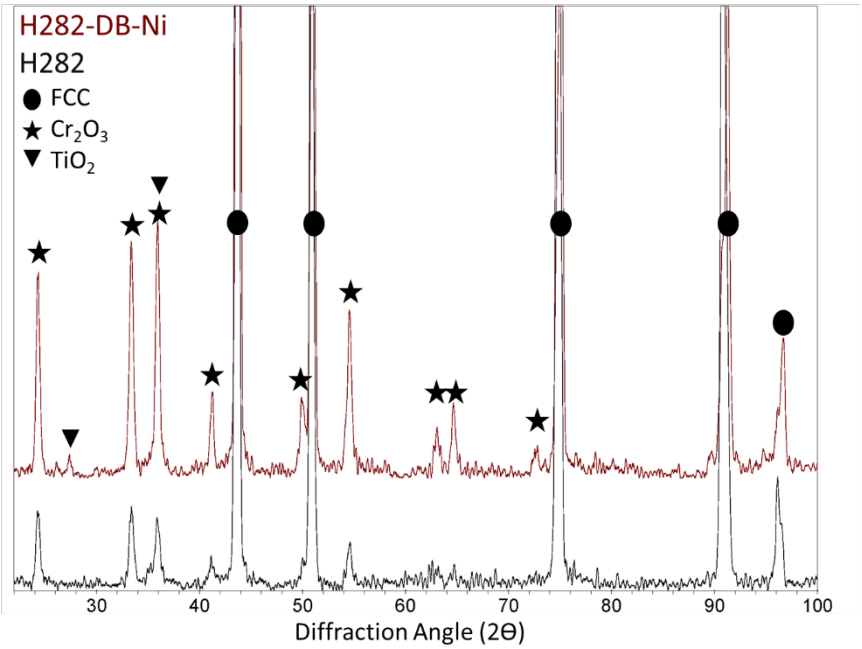

Figure 3: XRD spectra from the exposed surfaces of H282 (black), and H282-DB-Ni (red).

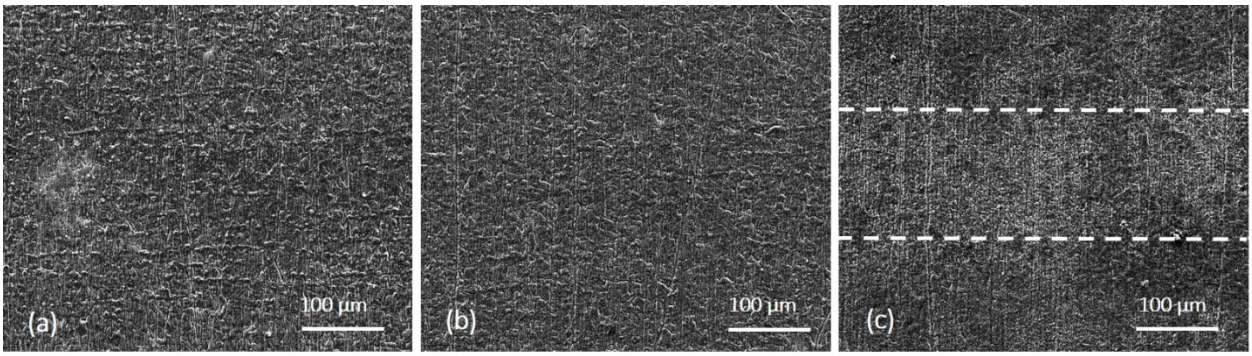

Figure 4: SEM secondary electron images of the exposed surfaces of the diffusion bonded coupons. (a) H230-DB-Ni, (b) H230-DB, and (c) H282-DB-Ni.

Fig. 4 shows surfaces of the exposed diffusion bonded coupons as observed in the secondary electron mode of the SEM. In all three cases, a dense scale with fine grains formed as a result of the 500 h CO_2 exposure at 700°C. In general, oxide grain size was finer (~1-5 µm) on the H282 coupons than the H230 coupons (~5-10 µm). Machining marks (as lines) can be seen through the thin oxide scale. Surface secondary electron imaging did not reveal any difference of the oxide scale between the bonded regions and away from the bonded regions on the H230 samples (Figs. 4a and b) whereas the H282 samples showed some contrast difference near the bonded regions as indicated with the dashed lines in Fig. 4c.

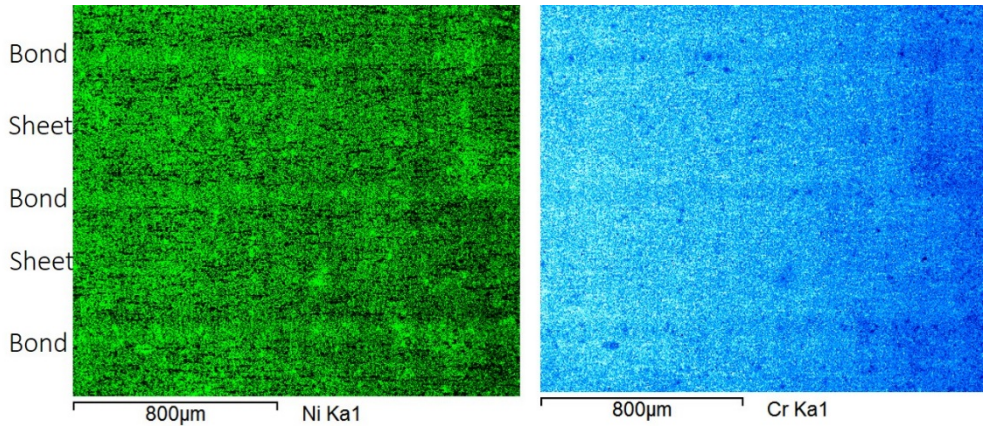

Figure 5: Slight Ni enrichment and Cr depletion were detected using x-ray elemental mapping on the bond regions of the H230-DB-Ni. The other elements did not show a detectable variation.

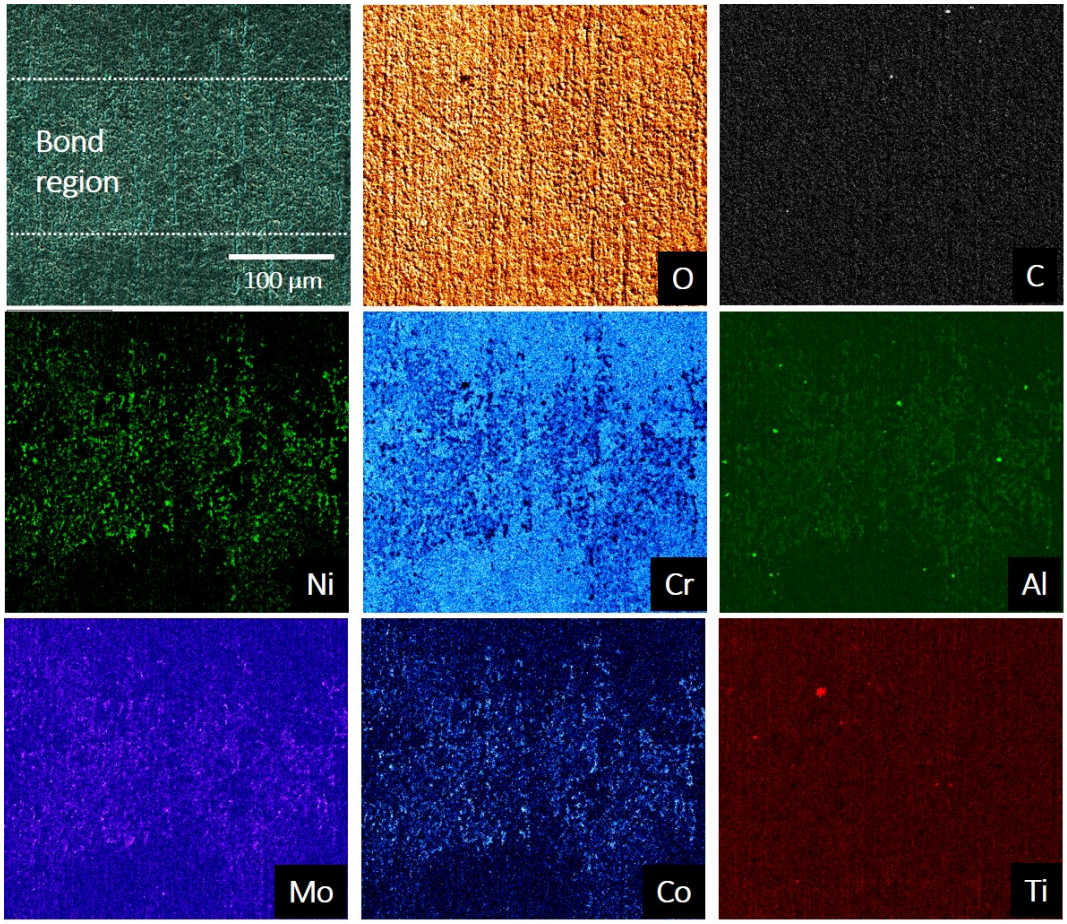

Figure 6: Elemental X-ray maps acquired on one of the bond regions of the H282-DB-Ni coupon after the 500 h CO_2 exposure at 700°C.

Elemental x-ray mapping using the SEM-EDS data performed on the top of the Cr_2O_3 scale on the H230-DB-Ni coupon showed a slight Ni enrichment and Cr depletion within the bond regions as depicted in Fig. 5. The other elements did not show any detectable variation between the bond and sheet regions. Conversely, elemental x-ray maps of the oxidized H282 coupons showed more variation in the elemental composition between the oxide scale on the bond regions and the oxide scale on the sheet material as shown in Fig. 6. While no variation in oxygen, carbon, and titanium was detected, there was an enrichment in nickel, aluminum, molybdenum, and cobalt in the scale on the bond regions. A depletion in chromium was also detected in the scale on the bond regions compared to the scale on the sheet material. More work is underway to understand whether these differences are in the oxide scale or they are reflecting the compositional difference between the sheet and bond in the substrate. It should be noted that microchemical analysis done on the unexposed samples of H230-DB-Ni and H230-DB did not show compositional difference between the bond region and sheet as reported by Kapoor et al. The same type of analysis is planned to be done on the unexposed H282-DB-Ni samples.

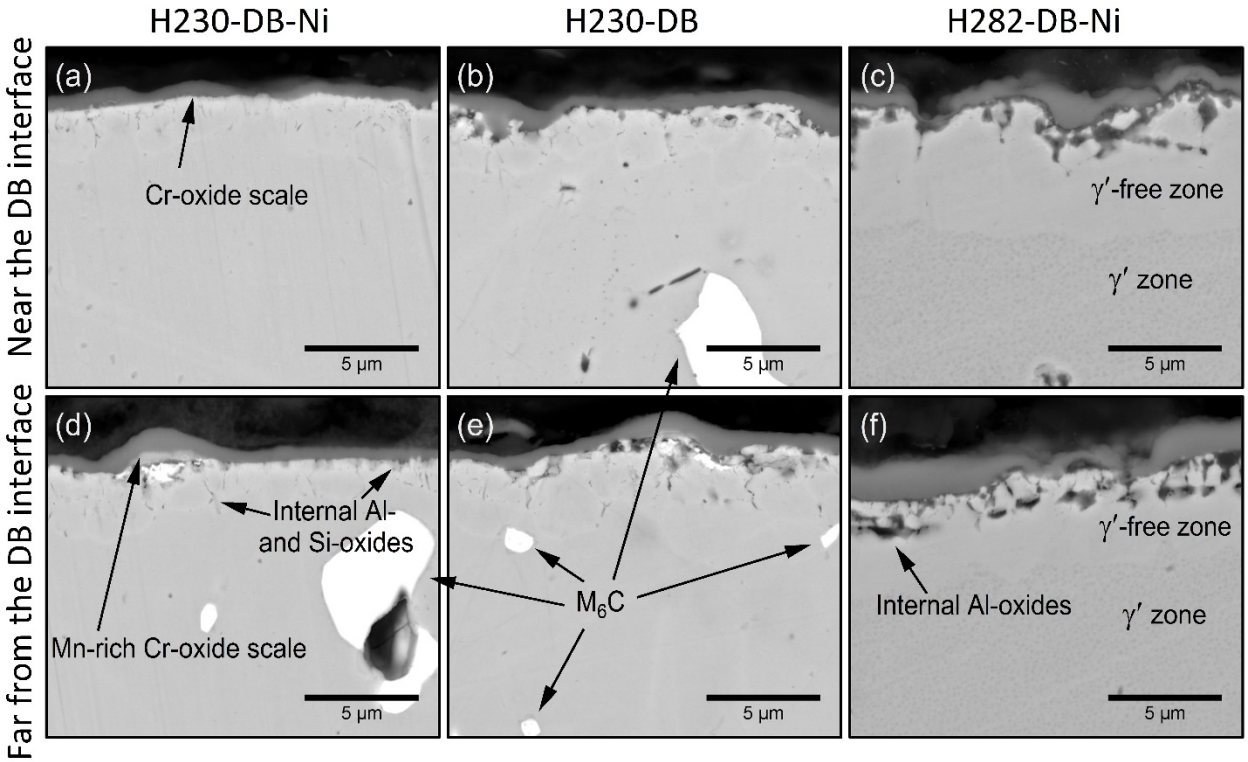

Figure 7: BSE micrographs showing cross-sections of three oxidized diffusion bonded (DB) samples near the DB interface and far (250 μm) from the DB interface. (a) H230-DB-Ni near the DB interface (b) H230-DB near the DB interface (c) H282-DB-Ni near the DB interface (d) H230-DB-Ni far from the DB interface (e) H230-DB far from the DB interface (f) H282-DB-Ni far from the DB interface.

Cross-section examination of the exposed diffusion bonded coupons using back-scattered electron (BSE) imaging revealed a thin oxide scale on all of the coupons (Fig. 7). The scale was approximately 0.5-1 µm thick on the H230 samples whereas it was slightly thicker (1-1.5 µm) on the H282 coupons. For H230 a thicker scale was observed above carbide particles near the sample surface. No significant thickness variation was observed between the scale on the bond and the scale on the sheet in either alloy.

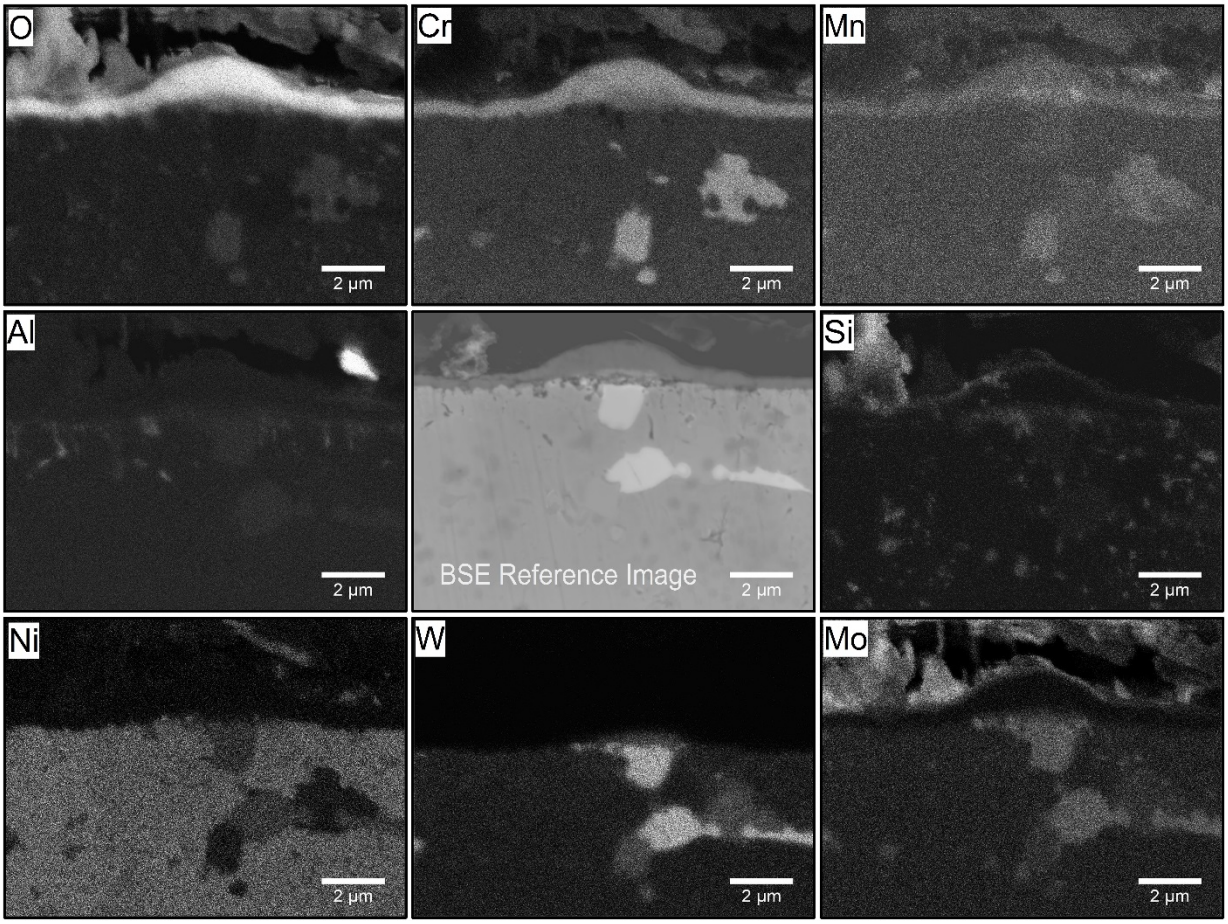

Figure 8: X-ray maps of select elements for H230-DB-Ni far from the DB interface. W and Si were acquired in WDS mode and all other elements were collected in EDS mode.

In order to identify the microstructural features observed in the sample cross-sections, X-ray mapping was performed on a representative area of H230-DB-Ni and H282-DB-Ni and the results are shown in Figs. 8 and 9, respectively. In both H230-DB-Ni (Fig. 8) and H282-DB-Ni (Fig. 9) the scale is primarily Cr-oxide, with a notable Mn content. A small amount of Si and Ti are observed at the scale interfaces in H230-DB-Ni and H282-DB-Ni, respectively. It should be noted that the mounting resin and polishing media used for sample preparation both contained Si and thus

some of the Si observed in Fig. 8 could be attributed to contamination. The region above the carbide particle at the surface of H230-DB-Ni is seen to contain a Mn-rich oxide layer between the carbide particle and the external scale, which may have contributed to the increased scale thickness in this region.

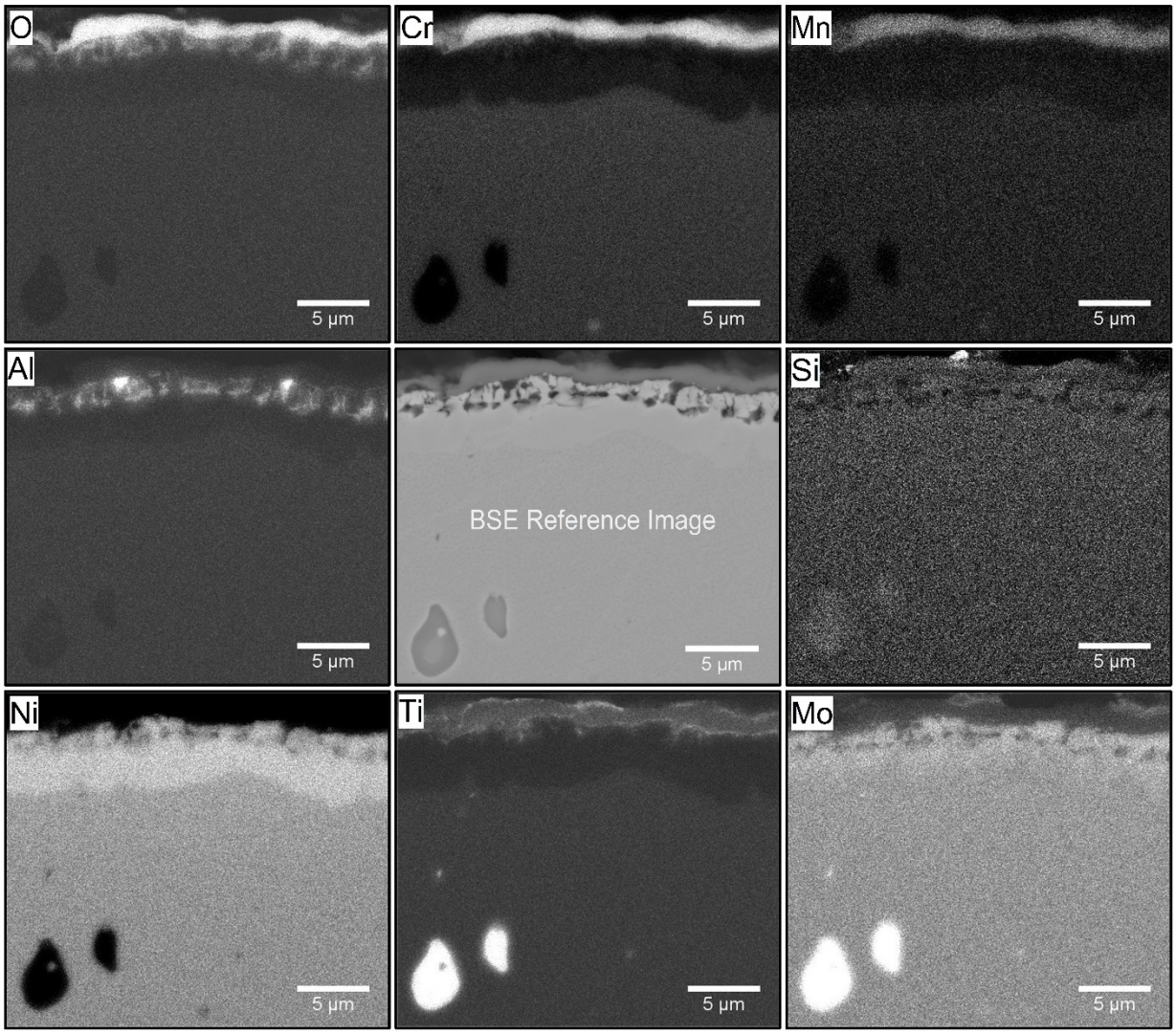

Figure 9: X-ray (EDS) maps of select elements for H282-DB-Ni far from the DB interface.

Internal oxidation was observed at varying extents. X-ray maps reveal that oxidized areas immediately beneath the scale are predominately Al-oxides for both alloys, while a small amount of internal Si-oxide and Ti-oxide is also observed in H230-DB-Ni and H282-DB-Ni, respectively. In general, both H230 diffusion bonded samples showed much less internal oxidation immediately beneath the scale than the H282-DB-Ni coupons. This was due to the increased levels of Ti and Al in H282 as compared to H230. Both Ti and Al are more reactive with oxygen than Cr, and so are

prone to form internal oxides beneath an external Cr_2O_3 scale. The internal oxidation was more pronounced on the grain boundaries and the majority of internal oxidation occurred within 1-2 µm into the metal. However, large precipitates of Cr-rich oxide were also observed adjacent to internal carbides near the sample surface in H230-DB-Ni up to 5 µm into the metal as seen in Fig. 8 (O, Cr, Mn maps). H282-DB-Ni showed an approximately 5 µm thick γ' precipitate-free zone below the external scale in both the diffusion bonded regions and sheet material. As seen in Figure 9, this zone is depleted of the metals that contributed to internal oxidation and scale formation (Cr, Mn, Al, Ti).

Diffusion bonding did not alter significantly the oxidation behavior of H230 material as determined after a 500 h exposure to CO_2 at 700°C. This was true whether the bonding was performed with or without Ni-plating. The oxidation scale exhibited similar characteristics and was continuous on the sheet and bond material of H230. Diffusion bonding of H282 (only tested with Ni-plating) resulted in increased mass gains during oxidation. However, a chromia scale was still formed, and overall oxidation rates were still low.

This study also confirmed that H230 was well bonded under the diffusion bonding conditions while H282 (not as homogenous as H230) requires modification of the diffusion bonding process.

Summary

As determined after a 500 h exposure to CO_2 at 700°C, diffusion bonding was not detrimental to the oxidation resistance of the H230. The diffusion bond regions of H230 did not exhibit an accelerated oxidation. This was not the case for the diffusion bonded samples of H282. Diffusion bonding of H282 resulted in increased mass gains during oxidation. However, a chromia scale was still formed, and overall oxidation rates were still low.

Acknowledgements

This work was performed in support of the U.S. Department of Energy's Fossil Energy Advanced Combustion Program. The Research was executed through NETL's Research and Innovation Center's Advanced Combustion Field Work Proposal (Richard Dennis and Daniel Driscoll, Technology Managers and Briggs White, Project Monitor). This research was supported in part by an appointment (RPO) to the National Energy Technology Laboratory Research Participation Program sponsored by the U.S. Department of Energy and administered by the Oak Ridge Institute for Science and Education. The authors would like to thank Joe Tylczak for the use of

High Temperature Laboratory for performing the exposure tests and Trevor Godell for sample preparation.

This report was prepared as an account of work sponsored by an agency of the United States Government. Neither the United States Government nor any agency thereof, nor any of their employees, makes any warranty, express or implied, or assumes any legal liability or responsibility for the accuracy, completeness, or usefulness of any information, apparatus, product, or process disclosed, or represents that its use would not infringe privately owned rights. Reference herein to any specific commercial product, process, or service by trade name, trademark, manufacturer, or otherwise does not necessarily constitute or imply its endorsement, recommendation, or favoring by the United States Government or any agency thereof. The views and opinions of authors expressed herein do not necessarily state or reflect those of the United States Government or any agency thereof.

References

Cook, G.O., Sorenson, C.D., "Overview of Transient Liquid Phase and Partial Transient Liquid Phase Bonding", Journal of Materials Science, 46 (2011) 5305-5323.

Foursprings, P.M., Nehrbauer, J.P., Sullivan, S., Nash, J., "Testing of Compact Recuperators For A Supercritical CO_2 Brayton Power Cycle", Proceedings of the 4th International Symposium on Supercritical CO2 Power Cycles, September 9-10, 2014, Pittsburgh, Pennsylvania, USA.

Ghazvini, M., Narayanan, V., "A Microscale Combustor Recuperator and Oil Heat Exchanger-Design and Thermofluidic Characterization", International Journal of Heat and Mass Transfer, 64 (2013) 988-1002.

Hill, A., Wallach, E.R., "Modelling Solid State Diffusion Bonding", Acta Metallurgica 37 (1989) 9 2425-2437.

Holcomb, G. R., Doğan, Ö.N., Carney, C., Rozman, K., Hawk, J.A., Anderson, M. H., "Materials Performance in Supercritical CO_2 in Comparison with Atmospheric Pressure CO_2 and Supercritical Steam, Proceedings of the 5th International Symposium on Supercritical CO2 Power Cycles, March 28-31, 2016, San Antonio, Texas, USA.

Kapoor, M., Doğan, Ö.N., Rozman, K., Hawk, J.A., Wilson, A., L'Estrange, T., Narayanan, V., "Diffusion Bonding of H230 Ni-Superalloy for Application in Microchannel Heat Exchangers", Proceedings of the 5th International Symposium on Supercritical CO2 Power Cycles, March 28-31, 2016, San Antonio, Texas, USA.

Lee, H. J., Kim, H., Kim, S. H., Jang, C., “Comparison of the Corrosion Behaviors of Fe-base and Ni-base Austenitic Alloys in High Temperature S-CO2 Environment,” Proceedings of the International Conference on Corrosion in Power Plants, EPRI-3002006972, Palo Alto, CA, 2015, pp. 3-47 to 3-63.

Le Pierres, R., Southall, D., Osborne, S., "Impact of Mechanical Design Issues on Printed Circuit Heat Exchangers," Proceedings of the 3rd International Symposium on Supercritical CO2 Power Cycles, May 24-25, 2011, Boulder, Colorado, USA.

Pérez-González, F.A., Garza-Montes-de Oca, N.F., Colás, R., “High Temperature Oxidation of the Haynes 282© Nickel-Based Superalloy,” Oxidation of Metals 82 (2014) 145-161.